European Geothermal Congress 2016
Strasbourg, France, 19-24 Sept 2016

A coupled thermo-hydro-geochemical modelling approach of the evolution of mineralogy in the EGS geothermal system at Soultz-sous-Forêts (France)

Yann Lucas[1], Viet Ngo[1], Alain Clément[1], Bertrand Fritz[1].

[1] UdS/EOST, CNRS, LHYGES, 1 rue Blessig 67084 Strasbourg Cedex

ylucas@unistra.fr

Keywords: Enhanced Geothermal System, Soultz-sous-Forêts (France), Thermo-hydro-geochemical modelling.

ABSTRACT

Operation of the enhanced geothermal system (EGS) requires to re-inject cooled fluid, after heat exchange at the surface to the energy production, into the geothermal reservoir. This cold re-injection triggers disequilibrium between fluid and rock and then implies the dissolution/precipitation of minerals, which may potentially cause changes in porosity, permeability, and flow pathways of the geothermal reservoir. As preliminary steps, we first studied the impact of changes in temperature by using a geochemical code (THERMA) which enables us to calculate the changes in equilibrium constants of all primary and secondary minerals and aqueous species as a function of temperature; then we performed numerical simulations in time at different temperatures, but without transport, to study the reaction pathways and to compare the thermodynamic and kinetic approaches in precipitation modelling (KINDIS code). These preliminary results enabled us to identify the key minerals, primary as well as secondary minerals among a large amount of tested minerals, and to get the necessary associated thermodynamic and kinetic data. The goal of what we present lies in the building of a coupled thermo-hydro-geochemical model of the EGS system. The temperature transport was implemented in the one dimensional coupled hydro-geochemical code (KIRMAT) by considering a classical temperature model, i.e. temperatures in fluid and rocks are equal. The simulations we performed with this coupled approach on the Soultz-sous-Forêts reservoir case made appear a great complexity of geochemical reactions, linked to the mineralogical complexity, especially sharp pH/Eh variations which may have a great impact on dissolution/precipitation conditions.

1. INTRODUCTION

The Soultz-sous-Forêts geothermal site located in Alsace, France, is an Enhanced Geothermal System (EGS). Local thermal gradients are high, up to 10°C/100 m in the upper part of the sedimentary section. The deep basement rock, referred to as "two-mica" granite (Hooijkaas et al 2006) and which is fractured and hydrothermally altered (Genter et al 2010) and contains large volumes of hot saline fluid (Gérard et al 2006). The Soultz geothermal system currently consists of three wells, GPK2, GPK3, and GPK4, which are used to test different production/injection strategies at different flow rates (Cuenot and Genter 2015) (Figure 1).

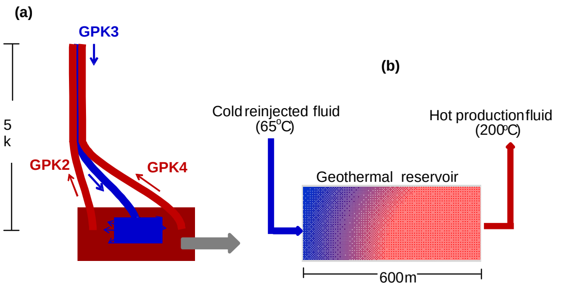

Figure 1: (a) Cross-section of the Soultz-sous-Forêts system with 3 wells that are currently exploited; (b) Conceptual model showing the temperatures of the re-injection well (≈ 65°C) and the production well (≈ 200°C).

The operation of the geothermal system requires continuous reinjection of the cooled fluid (about 65°C) into the geothermal reservoir. As a result, the re-injected brine flows through the fractures within the granite, inducing thermal and chemical disequilibrium between the fluid and the solid phase, potentially leading to the dissolution/precipitation of minerals. The possible mineralogical transformations have been characterized in numerous experimental investigations (e.g. Dubois et al 2000; Baldeyrou-Bailly et al 2004; Sausse et al 2006; Bartier et al 2008; Ledésert et al 2010; Hébert and Ledésert 2012) and predicted by several numerical calculations (Komninou and Yardley 1997; Rabemanana et al 2003; Bächler and Kohl 2005; André et al 2006; Fritz et al 2010).

In the framework of the Soultz geothermal system, a large set of data has been acquired by multidisciplinary approaches. However, the development and exploitation of the Soultz EGS system still faces various scientific and technical challenges (Genter et al 2010). Among them, the physical, chemical, and mechanical processes dominant in the Soultz reservoir remain poorly understood. The use of experimental approaches could be useful but are limited when applied in the context of the EGS system because of technical and cost issues. Alternatively, understanding of the EGS system can be advanced using a fully coupled thermo-hydro-geochemical model. For the Soultz system, there are only a few studies (Komninou and Yardley 1997; Rabemanana et al 2003; Bächler and Kohl 2005; André et al 2006), which investigated the fluid-rock interactions and their possible influence on the physical and transport properties within the geothermal reservoir. These previous studies are useful in terms of predicting the geochemical processes. However, the validity of these studies remains limited due to several reasons including their use of incomplete, poorly representative mineral assemblages. The limited number of minerals in the previous studies is explained by the fact that there were incomplete thermodynamic data related to Al^{3+}, Mg^{2+} and Fe^{2+} at high temperature (Bächler and Kohl 2005; André et al 2006) for estimating the activity coefficient using the Pitzer approach.

The literature review showed that illites, which are the characteristic minerals of the hydrothermal mineral assemblages (Bartier et al., 2008; Hébert et al 2010) are among the most important minerals in the Soultz reservoir. Their volume fraction can approximately reach 50% of the rock. The selection of mineral assemblages and their accurate thermodynamic data play a critical role in the accuracy of the output predictions.

Up to date research on mineralogy in the Soultz granite generally focuses on core samples. These previous studies provide an important knowledge of the mineralogical characteristics of the reservoir; two main types of alteration have been identified in propylitic and vein alteration assemblages. The propylitic alteration occurs in the granitic matrix and is characterized by replacement of biotite and hornblende by chlorite and transformation of plagioclase into illites, epidote, and hydrogarnet (Ledésert et al 2010). This alteration takes place over large scales and does not visibly modify the permeability and texture of the basement rock (Hooijkaas et al 2006).

The vein alteration resulting from water-rock interactions occurs locally in the fracture networks and can strongly modify the porosity and mineralogy of the granite. Vein alteration is characterized by the dissolution of primary minerals such as plagioclase and biotite, and the precipitation of secondary minerals, most commonly like calcite, clay minerals, and quartz. The mineralogy of the three wells in the Soultz system is highly heterogeneous making it difficult to accurately predict the mineralogy throughout the whole reservoir (Hébert et al 2010). This difficulty contributes to the limited validity of previous coupled thermo-hydro-chemical model for predicting the EGS system behaviour and performance.

2. MINERALOGICAL AND FLUID DATA

Special attention was paid to the mineral assemblage (Table 1) and behavior of minerals. Indeed, the appropriateness of the mineral assemblage of the developed model generally plays a critical role in the modeling results. Secondly, depending on the location, the contact between the cold re-injected fluid at about 65°C and granitic rock initially at 200°C causes decrease in the temperature of the reservoir fluid, which is the primary driver of changes in behavior of minerals

Table 1: Mineral assemblage. Plagioclase was replaced by albite and anorthite end-members. A group of K-muscovite, annite, and phlogopite was used for mica. Chlorite was represented in terms of clinochlore and chamosite end-members. Illites are represented by Fe-illite, Mg-illite, and Al-illite.

Minerals	Structural formula	Volume fraction (%)
Quartz	SiO_2	25.87
K-Feldspar	$KAlSi_3O_8$	22.63
Albite	$NaAlSi_3O_8$	36.25
Anorthite	$Ca(Al_2Si_2)O_8$	2
K-Muscovite	$KAl_2(AlSi_3)O_{10}(OH)_2$	2.82
Annite	$KFe_3(AlSi_3)O_{10}(OH)_2$	2.82
Phlogopite	$KMg_3(AlSi_3)O_{10}(OH)_2$	2.82
Calcite	$CaCO_3$	0.46
Mg-Illite	$K_{0.85}Mg_{0.25}Al_{2.35}Si_{3.4}O_{10}(OH)_2$	0.87
Fe-Illite	$K_{0.85}Fe_{0.25}Al_{2.35}Si_{3.4}O_{10}(OH)_2$	0.87
Al-Illite	$K_{0.85}Al_{2.85}Si_{3.15}O_{10}(OH)_2$	0.87
Smectite	$[Ca_{0.009}Na_{0.409}K_{0.024}][(Si_{3.738}Al_{0.262}]$ $[Al_{1.598}Fe_{0.208}Mg_{0.214}]O_{10}(OH)_2$	0.97
Dolomite	$CaMg(CO_3)_2$	0.08
Pyrite	FeS_2	0.07
Galena	PbS	0.13
Chamosite	$Fe_5Al(AlSi_3)O_{10}(OH)_8$	0.24
Clinochlore	$Mg_5Al(AlSi_3)O_{10}(OH)_8$	0.24

This modeling work is based on the assumption that the mineralogical composition is the same throughout the whole Soultz geothermal reservoir, and the reaction between the geothermal brine and the Soultz granite occurs under decreasing temperatures from 200°C to 65°C (Figure 1). To our knowledge, there are no detailed analysis describing how CO_2 and O_2 gas evolve during exploitation; therefore, simulation runs were carried out with both open and closed systems, i.e., CO_2 and O_2 partial pressures are freely changed or fixed, respectively. Fixed CO_2 and O_2 partial pressures mean that the system will be buffered for the carbonate and the Eh-pH systems, respectively. Varying partial pressures are equilibrium values for CO_2 and O_2 based on calculated aqueous speciation. The numerical calculations performed in this manner are able to distinguish the effect of CO_2 and O_2 partial pressures on the evolution tendency of the system.

The chemical composition and physical characteristics of the re-injected fluid are reported in Table 2. Regarding the physical characteristics used in the current study, the value of 117 mV for the redox potential determined in the laboratory scale by Scheiber et al (2013) was not reliable for the saline fluid at 200°C in the geothermal reservoir. Therefore, this parameter was assessed (assed ?) using the value of -250 mV determined via the thermodynamic modeling by Fritz et al (2010). pH of the saline fluid was estimated around 4.8. The CO_2 partial pressure was also estimated by the equilibrium calculation as reported in the study of Sanjuan et al (2006).

Table 2: pH, Eh, and chemical composition of the re-injection fluid, which was determined from the measurement in the laboratory scale of the production well (Sanjuan et al., 2006; Scheiber et al., 2013) and thermodynamic modeling (Fritz et al., 2010).

pH	4.82
Eh (mV)	-250
pCO_2 (atm)	2
Elements	*Concentration (mol/kgH2O)*
Na	1.20E+00
K	8.31E-02
Ca	1.72E-01
Mg	5.14E-03
Si	7.11E-03
Al	1.85E-06
Fe	1.79E-04
Pb	1.48E-06
S	6.14E-04
Cl	1.66E+00
Alkalinity (meq $kg^{-1}H_2O$)	5

3. IMPACT OF TEMPERATURE CHANGES

3.1 Calculation procedure

The simulations were carried out using the THERMA code (Fritz, 1981) that involves equations describing the conservation of solute mass, ionic strength, electrical neutrality, and thermodynamic constant of minerals. For the aqueous species and minerals in the targeted system, the THERMA code describes the equilibrium relationship as:

$$K_j = \prod_{i\in B}[\alpha_i]^{\beta_{ij}} = \prod_{i\in B}[m_i\gamma_i]^{\beta_{ij}} \qquad [1]$$

Where K_j is the equilibrium constant of the compound j, α_i is the activity of species i, m_i is the molality, γ_i is the activity coefficient, B is the basic species assemblage of the system, β_{ij} is the stoichiometric coefficient of species i in the compound j. The equilibrium constant K_j can be expressed as a function of the N_i mole number of species i as:

$$\log K_j = \sum_{i\in B}\beta_{ij}\left[\log N_i + \log\gamma_i - \log\left(N_{H_2O}\right)\right] \qquad [2]$$

The first and second orders of the derivative of K_j as a function of temperature are given, here at first order:

$$\frac{d\log K_j}{dT} = \frac{1}{\ln(10)}\sum_{i\in B}\beta_{ij}\left[\frac{N_i^{'}}{N_i} + \frac{d\ln\gamma_i}{dT} - \frac{N_{H_2O}^{'}}{N_{H_2O}}\right] \qquad [3]$$

In the current study, the activity coefficient γ_i is calculated using the extended Debye-Huckel model (Debye and Hückel, 1923):

$$\log\gamma_i = -\frac{Az_i^2\sqrt{I}}{1+\alpha_i^0 B\sqrt{I}} + CI \qquad [4]$$

Where A, B, and C are the Debye-Huckel constants, α_i^0 is the size of the species i, I is the ionic strength of the solution, and z_i is the electric charge of the species i.

These equations are solved according to the following method (Figure 2):

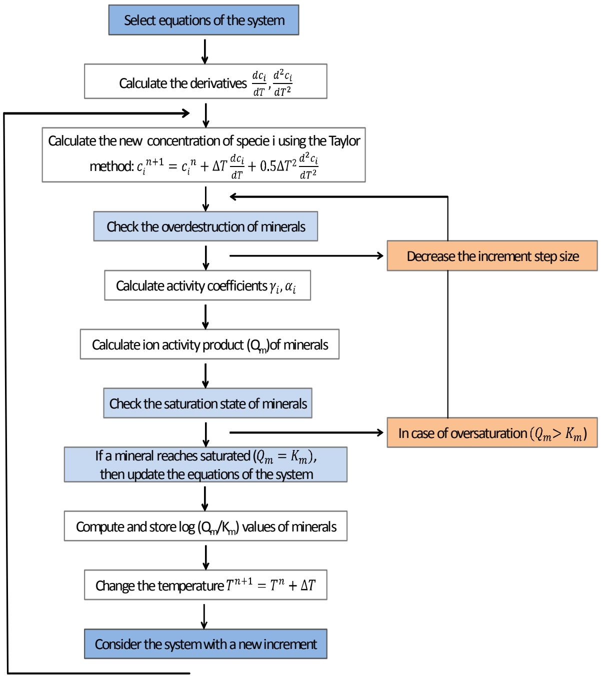

Figure 2: Flowchart of the scheme implemented in the THERMA code to study the saturation state of the minerals in the system.

The activity coefficient can be computed using the extended Debye-Huckel (Debye and Hückel 1923) and/or Pitzer (Pitzer 1973) approaches. The former is widely used for geochemical modeling but is less adequate for the current study due to the high salinity of the Soultz fluids. Within the framework of the EGS Soultz system, three modeling efforts (Rabemanana et al 2003; Bächler and Kohl 2005; André et al 2006) have utilized the Pitzer approach to calculate the activity coefficient because it better estimate the activity coefficient than the Debye-Huckel approach. However, its application raises several issues such as the lack of parameters for $Al3^+$, Mg^{2+}, and Fe^{2+} at high temperatures (Durst and Vuataz 2000; Rabemanana et al 2003; Bächler and Kohl 2005; André et al 2006). This prevents adequate modeling for the clay minerals, especially illites, which [2] are among the most important minerals in the Soultz reservoir. As a consequence, these modeling studies did not account for illites. However, according to Durst and Vuataz, (2000), the use of the Pitzer approach can also increase the complexity of the code and decrease the performance of the model. This problem cannot be ignored when modeling the EGS system, because it requires strongly coupled physical and chemical processes. Accordingly, in the present study, we use the extended Debye-Huckel equations in order to model illite behavior while avoiding the disadvantages of the Pitzer approach. In the Soultz system the ionic strength of the aqueous solution is buffered at a value near 1.5. Ionic strength does not vary significantly, so the errors associated with the Debye-Huckel approach, for some ion activity values, will be constant.

3.2 Results

The evolution of element concentrations over a temperature range of 65^{o}C to 200^{o}C is presented in Figure 3. Regarding the open system, the model predicted that the cooling process resulted in the decrease in Ca (not appearing clearly due to the large scale of y- axis), Si, and Al concentrations (Figure 3), but the concentrations of other constituents such as K, Na, Mg, and Pb remained almost constant. The changes in Ca, Si, and Al contents were controlled by the dissolution and precipitation of some major minerals, including calcite, quartz, illites. A further analysis of modeling results indicated that the logarithm of oxygen fugacity decreased from -38 to -57, while that of CO_2 slightly changed from 0.31 to 0.37 (not shown in Figure 3). In addition, the pH and redox potential have tendency of becoming less acidic and more positive, respectively.

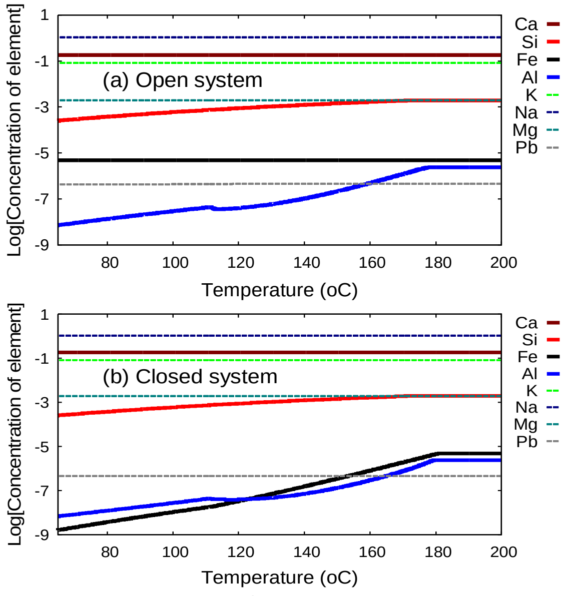

Figure 3: Evolution of Ca, Si, Fe, Al, K, Na, Mg, and Pb concentrations (mol/kgH2O) as a function of temperature in two systems: (a) open system, where the numerical calculations assume that CO2 and O2 partial pressures freely changed; (b) closed system, in which CO2 and O2 partial pressures are fixed during the simulations.

When the CO_2 and O_2 partial pressures were fixed during the simulation (closed system), the modeling results showed that the evolution of chemical elements in this case was almost similar to those of the open system. The only difference is related to the evolution of Fe, meaning that this constituent was decreased significantly in the closed system, whereas it was constant in the open system. This suggests that the assumption of whether the gas pressures were freely changed and/or fixed, has a direct effect on the evolution of minerals containing Fe.

The thermodynamic modeling predicted that calcite (Figure 4) and dolomite had tendency of approaching the equilibrium state when the system was cooled down, but only calcite reached equilibrium with the saline solution while dolomite remained slightly undersaturated (Ngo et al 2016).

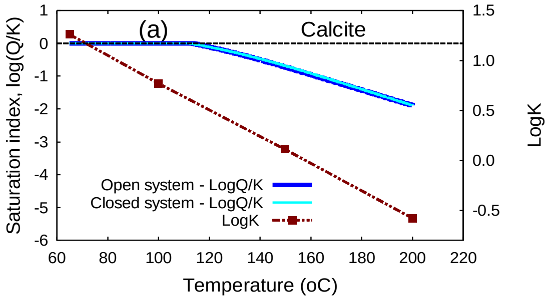

Figure 4: Mineral saturation indices (log (Q/K)) of calcite as a function of the temperature using the THERMA code, as well as the corresponding solubility.

For the high temperature range (200^{o}C-180^{o}C), the used saline solution was slightly undersaturated with respect to Fe-illite, Mg-illite, Al-illite, smectite and clinochlore. With respect to the intermediate temperature range of 180^{o}C-110^{o}C, clinochlore remained saturated along this temperature range, whereas the degree of saturation of 3 illites and smectite was dropped smoothly and then increased again. This suggests that there is a competition between chlorite (here for example clinochlore) and illite/smectite to be formed when the geothermal brine reacts with the granitic rock. While cooling from 110^{o}C to 65^{o}C, three illites remained always or nearly in equilibrium with the brine solution. In contrast, the saturation degree of smectite and clinochlore decreased, in particular for the case of clinochlore. This may indicate that for the cold temperature range, illites are more likely precipitated, instead of clinochlore or smectite. Another interesting point is that for the high and intermediate temperature ranges the calculated SI of three illites were very close to each other, also suggesting that there is possibly competition between these illites in the system (Ngo et al 2016).

Except at the high temperature, the saline solution is in equilibrium with respect to quartz along the cooling direction. The computed saturation index of K-feldspar was also distinguished in three main parts, meaning that increased in the high temperature range (200^{o}C-180^{o}C); slightly decreased and then increased in the intermediate temperature range (180^{o}C–110^{o}C);

remained saturated in the low temperature range (110^{o}C-65^{o}C). The evolution of saturation index of albite was quite similar to the one of smectite in terms of the trend corresponding to three temperature ranges.

The saturation indexes of six other minerals (anorthite, K-muscovite, annite, chamosite, pyrite, and galena) were calculated. The saturation index was quite similar between the open and closed systems for two minerals anorthite and K-muscovite. But this evolved very differently between the two systems for annite, chamosite, pyrite (Figure 5), and galena, as resulted in the differences in concentrations of Fe and S when the system was supposed to be open or closed. Four minerals such as anorthite, K-muscovite, annite, and chamosite were always unsaturated under the Soultz conditions when the reservoir was cooled down. In contrast, pyrite and galena reached equilibrium when the temperature of the open system was cooled down to about 110^{o}C, whereas their degree of saturation in the case of the closed system went very far from the equilibrium state.

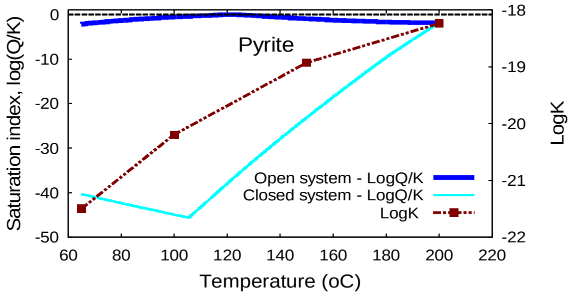

Figure 5: Mineral saturation indices (log (Q/K)) of Pyrite as a function of the temperature computed using the THERMA code, as well as the corresponding solubility.

Altogether, the previously reported saturation indexes of reservoir minerals showed that among the carbonates, calcite had a great possibility to be formed, while for the silicate group illite/smectite and quartz were highly favored to precipitate. In addition, other minerals such as clinochlore, K-feldspar, pyrite, and galena were also likely formed following the cooling direction of the geothermal reservoir. The other minerals initially present in the fresh granite such as anorthite, K-muscovite, annite were always undersaturated, and thereby they are probably continuously transformed into the main hydrothermal alteration products such as calcite, illites, and quartz. These findings are consistent with both experimental and modeling results (Komninou and Yardley 1997; Rabemanana et al 2003; Bächler and Kohl 2005; André et al 2006; Fritz et al 2010).

The comparison of the modeling results obtained from two cases (open and closed systems) also indicated that the approaches in which gas pressures may freely vary or remain fixed during the simulations only influence the saturation indexes of Fe rich minerals and Fe content in the EGS Soultz system, whereas those of other minerals, together with the evolution of other chemical constituents evolved very similarly. Regarding the modeling results for both approaches, only the approach assuming open system predicted the precipitation of sulfides. Thus, this finding, along with the above conclusion reported from the modeling results, can help to identify that what we call here the open system approach may be more appropriate for predicting the geochemical evolution in the Soultz reservoir.

3. TIME EVOLUTION

In this part, we study the evolution in time of the system at different temperatures (200°C, 100°C and 65°C) and, in a first approach, we quantify this evolution with the KINDIS code (Madé et al 1994). Dissolution was treated kinetically, and precipitation thermodynamically (= at equilibrium) or kinetically.

3.1 Equations and data

The KINDIS code uses the following expression to describe the mineral dissolution (Lasaga et al 1994):

$$r_d = k_d S\left[\left(\frac{Q}{K}\right)^m - 1\right]^n \qquad [5]$$

Where r_d (mol year^{-1} kg^{-1}$_{H2O}$) is the dissolution rate; k_d (mol.m^{-2}.year^{-1}) is the dissolution rate constant; S (m^2.kg^{-1}$_{H2O}$) is the surface area; Q is the activity product; K is the thermodynamic equilibrium constant at the given temperature (Table 3), m and n are empirical exponents.

Table 3: Thermodynamic database of the three more important primary minerals in the Soultz granite tested in the simulations. (Blanc et al 2012).

Minerals	LogK 200^{o}C	LogK 100^{o}C	LogK 65 ^{o}C	Molar volume (cm^3.mol^{-1})
Primary minerals				
Quartz	-2.34	-2.98	-3.3	22.69
K-Feldspar	-3.74	-1.94	-1.13	108.74
Albite	-2.93	-0.21	1.01	100.07

For the practical application of the dissolution law, the temperature dependence of the rate constant is described using the Arrhenius equation, which can be expressed in general form as following (Madé et al 1994; Palandri and Kharaka 2004):

$$k_d = \left[\begin{array}{l} k_{25}^{Acid}\exp\left[\frac{-E_a^{Acid}}{R}\left(\frac{1}{T}-\frac{1}{298.15}\right)\right]\alpha_{Acid}^{n_{Acid}} \\ +k_{25}^{Neutral}\exp\left[\frac{-E_a^{Neutral}}{R}\left(\frac{1}{T}-\frac{1}{298.15}\right)\right] \\ +k_{25}^{Base}\exp\left[\frac{-E_a^{Base}}{R}\left(\frac{1}{T}-\frac{1}{298.15}\right)\right]a_{Base}^{n_{Base}} \end{array}\right] \qquad [6]$$

where k_{25}^{Acid}, $k_{25}^{Neutral}$, k_{25}^{Base} (mol.m^{-2}.year^{-1}) are the dissolution rate constants at 25°C and pH = 0, which correspond to the acid, neutral, and basic pH zones, respectively; E_a^{Acid}, $E_a^{Neutral}$, E_a^{Base} (J.mol^{-1}) are the activation energies with respect to the acid, neutral, and basic zones, respectively; n_{Acid} and n_{Base} (-) are reaction orders with respect to the pH of the solution; R (J.K^{-1}.mol^{-1}) is the gas constant ; T (K) is the temperature. Some values of kinetical parameters are given in Table 4.

Table 4: Kinetic constants of dissolution reaction at 25°C for the three main primary minerals of the Soultz granite.

	Quartz	K-Feldspar	Albite
k_a (mol. m^{-2} .year-1)	1.44E-4	2.75E-3	2.18E-03
k_n (mol m-2 year-1)	1.44E-6	1.23E-5	8.69E-06
k_b (mol m-2 year-1)	1.62E-9	1.99E-14	7.92E-09
pH_a	4.0	4.7	6
pH_b	5.9	10.7	8
n_a	0.50	0.50	0.46
n_b	-0.50	-0.82	-0.57
E_a (K.J. mol-1)	99.2	51.7	65
E_n (K.J. mol-1)	90.1	38	69.8
E_b (K.J. mol-1)	108.4	94.1	71

The precipitation of a mineral can also be described by using a kinetic approach. The KINDIS code describes the precipitation rate of a mineral according to the following expression:

$$r_p = k_p^{25}\exp\left[\frac{-E_a}{R}\left(\frac{1}{T}-\frac{1}{298.15}\right)\right]S\left[\left(\frac{Q}{K}\right)^p-1\right]^q \qquad [7]$$

Where k_p is the kinetic rate constant of precipitation (mol.m^{-2}.year^{-1}), p and q are experimental values describing the dependence of the reaction on the saturation state. These parameters have been collected for all the potentially used minerals and are partially presented in Table 5:

Table 5: Kinetic constants of precipitation reaction of three main primary minerals at 25 °C.

Minerals	Kinetic constants	p	q	Ea
	(mol m^{-2} year^{-1})			(KJ mol^{-1})
Quartz	*2.65E-4*	*1*	*1*	*50*
Calcite	*2.93E+0*	*0.5*	*2.0*	*80*
Mg-Illite	*1.73E-5*	*1*	*1*	*66*
Fe-Illite	*1.73E-5*	*1*	*1*	*66*
Al-Illite	*1.73E-5*	*1*	*1*	*66*

As it appeared in Equations 5 and 7, the reactive surface area of primary minerals is a sensitive parameter when the dissolution of mineral is controlled by the surface reaction. In general, the reactive surface area of mineral changes over the course of the dissolution/precipitation process as a feed-back effect of this process. The application of geochemical modeling tools requires estimation of the reactive surface area for all primary minerals. In the literature, modelers usually identify the reactive surface area with the BET, the edge site or the geometric surface area. The BET values have been collected for all the potentially used minerals and are partially presented in Table 6:

Table 6: Reactive surface area of the three main primary minerals in the Soultz granite which are estimated from the BET area value and the mineralogical composition.

Minerals	BET area	Reactive surface area
	(m^2 .g^{-1})	(m^2 .kg^{-1}H_2O)
Quartz	0.05^a	308
K-Feldspar	1.43^b	7457
Albite	0.83^c	8263

3.2 Results

All the collected data enabled us to perform simulations in order to get information about the mineralogical evolution from a qualitative and quantitative point of view at different temperatures. As shown in Figure 6 concerning the phase relations at 65°C for CaO-CO2-FeO-MgO plotted using log[a(Ca2+)/a2(H+)] and log[a(HCO3-)/a(H+)], the CaO-CO2-FeO-MgO activity diagram depicts three main carbonates such as calcite, dolomite and siderite. It can be seen from this diagram that calcite stability field is favored by the high activity of Ca2+, while that of dolomite is located in the zone corresponding to the low activity of Ca2+ and the high activity of HCO3-. The stability field of siderite is characterized by the relatively low activity of Ca2+ and low activity of HCO3-. This diagram clearly shows that under the Soultz conditions, the aqueous solution chemistry is located in the stability field of calcite. The interaction between geothermal brine and rock in the reservoir induces the relationship of log[a(Ca2+)/a2(H+)] and log[a(HCO3-)/a(H+)] evolving towards the higher activity of Ca2+ due to the dissolution of the rich-Ca minerals, whatever the chosen modeling scenario.

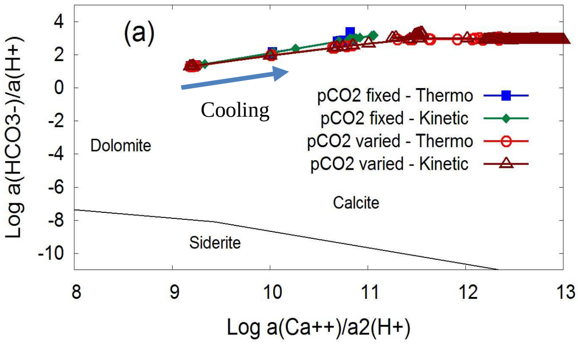

Figure 6: Activity diagrams showing the phase relations at 65 °C for (a) system CaO-CO_2-FeO-MgO, plotted as the activity of $[Ca^{2+}]/[H^+]^2$ versus $[HCO_3^-]/[H^+]$.

Simulations also enable us to quantify production of several minerals such as calcite, illites, smectite, clinochlore, K-feldspar, and quartz. In Figure 7, calcite production is shown at different temperatures, using thermodynamical or kinetical modes, with fixed or varied pCO2. Differences can be significant.

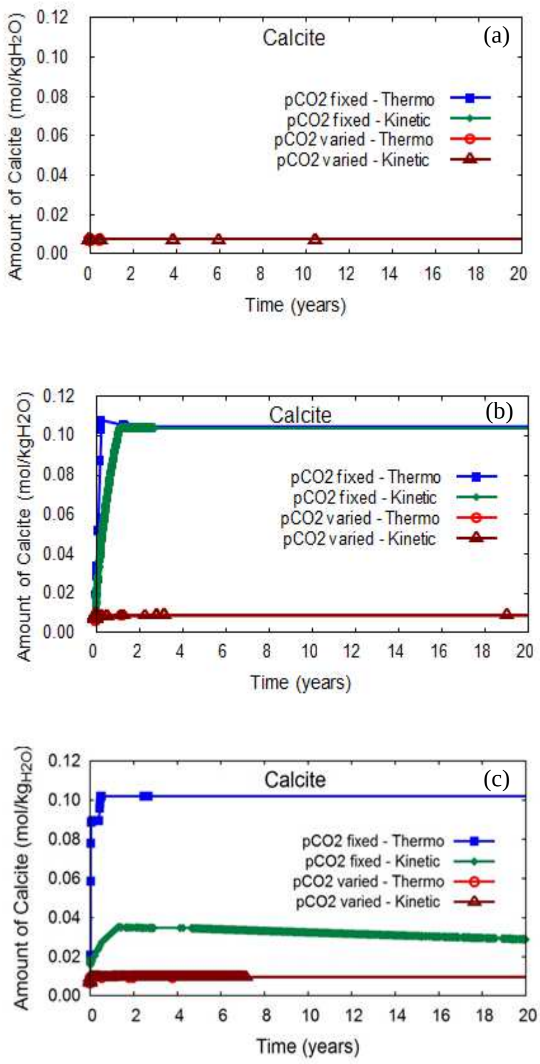

Figure 7: Evolution of calcite amount at: (a) 200°C; (b) 100°C; (c) 65°C, simulated by the KINDIS code.

4. COUPLED APPROACH

4.1 Equations and data

The KIRMAT code (Gérard et al 1998) is a one-dimensional coupled hydrogeochemical code based on the previous geochemical code KINDIS. The aim of this part is to develop a coupled thermo-hydrogeochemical model in the framework of the conceptual model shown in Figure 1. First we had to introduce heat transport in KIRMAT. We used the classical one-temperature model (Ledoux 1978; Sauty 1982):

$$(\rho c)_{MP}\frac{\partial T}{\partial t} = div\left(\lambda' \vec{grad}(T) - (\rho c)_{Fluid}\, T.\vec{U}\right) \quad [8]$$

where $(\rho c)_{MP}$ is the porous medium thermic capacity ($J.kg^{-1}.K^{-1}$), T temperature (K), λ' the equivalent thermic conductivity ($W.m^{-1}.K^{-1}$), $(\rho c)_{Fluid}$ is the fluid thermic capacity ($J.kg^{-1}.K^{-1}$), $\vec{U}$ the Darcy's velocity. $(\rho c)_{MP}$ is calculated as follows:

$$(\rho c)_{MP} = \omega(\rho c)_{Fluid} + (1-w)(\rho c)_{Solid} \quad [9]$$

where $(\rho c)_{Solid}$ is the solid thermic capacity ($J.kg^{-1}.K^{-1}$) and ω the total porosity. λ' is calculated as follows:

$$\lambda' = \lambda_{MP} + (\rho c)_{Fluid} D \quad [10]$$

where λ_{MP} is the porous medium thermic conductivity ($W.m^{-1}.K^{-1}$) and D ($m^2.s^{-1}$) a thermic dispersion similar to tracer dispersion.

The heat transport equation 8 can be solved independently from transport and reaction equations, but temperature has to be coupled with all parameters which depend on it (thermodynamic as product solubility, kinetic as dissolution rate constant), which therefore have been set as function of temperature.

4.2 First Simulations

To test our code, we have built a model of three meshes of ten meters. Darcy's velocity is 315 $m.year^{-1}$ and porosity 10%. The initial fluid has a temperature of 200°C and the injected fluid is at 65°C. As shown in Figure 8, we have checked that temperature evolution is correctly simulated in the framework of used thermic parameters.

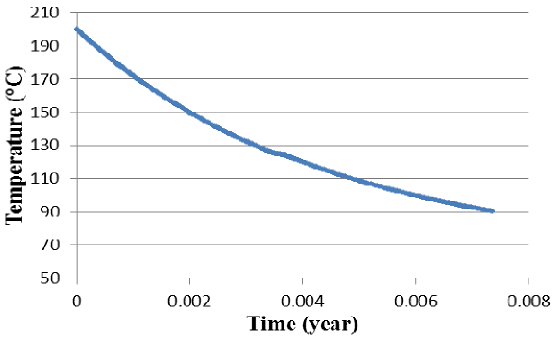

Figure 8: Temperature evolution in time on the first ten meters of a simplified model.

About geochemical part, we have used 14 primary minerals and tested 40 possible secondary minerals. On this simplified model, simulations have highlighted several numerical problems linked to geochemical complexity and high disequilibrium caused by a sharp temperature change, as alternate of destruction, till total destruction, and precipitation of some minerals.

In Figure 9 we present some results in the first mesh, on about two days. It is shown that sensible parameters as pH and Eh sharply change. Redox conditions play a major role on the presence of sulfate ions, which also sharply vary.

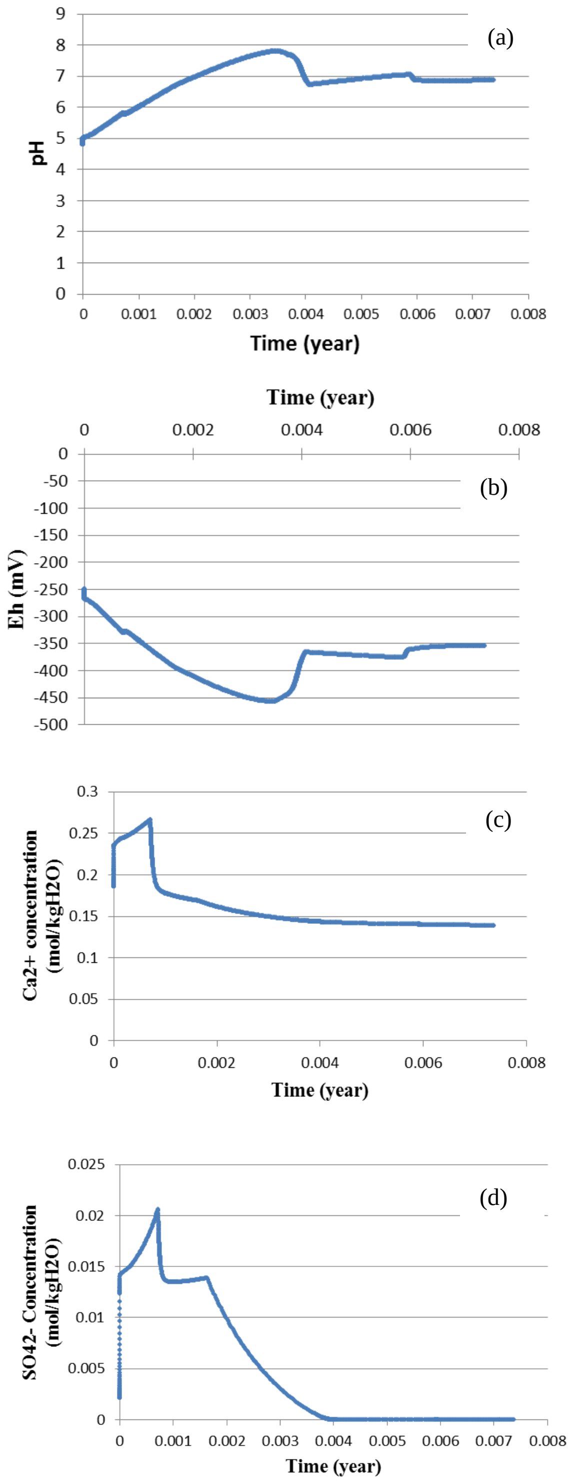

Figure 9: Some results from a simulation on 2 days: (a) pH; (b) Eh; (c) Ca^{2+} concentration; (d) $SO4^{2-}$. Sharp variations cause numerical problems which made simulation last about two days.

5. CONCLUSIONS

The three steps of our approach have enabled us: (i) to identify the main minerals which are likely to play a significant role in the mineralogical evolution of the Soultz reservoir; (ii) to collect the thermodynamic and kinetic corresponding data in function of temperature and to test different scenarios concerning thermodynamic/kinetic precipitation and varied/fixed pCO2; (iii) to build a first coupled thermo-hydrogeochemical model, which needs to be improved.

REFERENCES

André, L., Rabemanana, V., Vuataz, F.D.. Influence of water-rock interactions on fracture permeability of the deep reservoir at Soultz-sous-Forêts, France. *Geothermics* (2006), **35**(5-6), 507-531.

Bächler, D., Kohl, T. Coupled thermal-hydraulic-chemical modelling of enhanced geothermal systems. *Geophysical Journal International* (2005), **161**(2), 533-548.

Baldeyrou-Bailly, A., Surma, F., Fritz, B. Geophysical and mineralogical impacts of fluid injection in a geothermal system: The Hot Fractured Rock site at Soultz-sous-Forêts, France. In: *Geological Society Special Publication* (2004), **236**, 355-367.

Bartier, D., Ledésert, B., Clauer, N., Meunier, A., Liewig, N., Morvan, G., Addad, A. Hydrothermal alteration of the Soultz-sous-Forêts granite (Hot Fractured Rock geothermal exchanger) into a tosudite and illite assemblage. *European Journal of Mineralogy* (2008), **20**(1), 131-142.

Blanc, P., Lassin, A., Piantone, P., Azaroual, M., Jacquemet, N., Fabbri, A., Gaucher, E.C. Thermoddem: A geochemical database focused on low temperature water/rock interactions and waste materials. *Applied Geochemistry* (2012), **27**(10), 2107-2116.

Cuenot, N., Dorbath, C., Dorbath, L. Analysis of the microseismicity induced by fluid injections at the EGS site of Soultz-sous-Forêts (Alsace, France): Implications for the characterization of the geothermal reservoir properties. *Pure and Applied Geophysics* (2008), **165**(5), 797-828.

Debye, P., Hückel, E. Zur theorie der elektrolyte. *Phys. Z.* (1923) **24**, 185-206.

Dubois, M., Ledésert, B., Potdevin, J.L., Vançon, S. Determination of the formation conditions of carbonates in an alteration zone of the Soultz-sous-Forêts granite (Rhine Graben): The fluid inclusion record. *Comptes Rendus de l'Académie de Sciences - Série IIa: Sciences de la Terre et des Planètes* (2000), **331**(4), 303-309.

Durst, P., Vuataz, F.-D.. Fluid-rock interactions in hot dry rock reservoirs. A review of the HDR sites and detailed investigations of the Soultz-sous-Forets system. In: *Proceedings World Geothermal Congress* (2000), Kyushu-Tohoku, Japan.

Fritz, B., 1981. Etude thermodynamique et modélisation des réactions hydrothermales et diagénétiques.. *Sci. Geol., Mém.* 65, 197p.

Fritz, B., Jacquot, E., Jacquemont, B., Baldeyrou-Bailly, A., Rosener, M., Vidal, O., 2010. Geochemical modelling of fluid-rock interactions in the context of the Soultz-sous-Forêts geothermal system. *Comptes Rendus - Géoscience* (2010), **342**(7-8), 653-667

Genter, A., Evans, K., Cuenot, N., Fritsch, D., Sanjuan, B. Contribution of the exploration of deep crystalline fractured reservoir of Soultz to the knowledge of enhanced geothermal systems (EGS). *Comptes Rendus - Géoscience* (2010), **342**(7-8), 502-516.

Gérard, F., Clement, A., Fritz, B., 1998 Numerical validation of a Eulerian hydrochemical code using a 1D multisolute mass transport system involving heterogeneous kinetically controlled reactions. *J. Contam. Hydrol* (1998), **30**, 201–216.

Gérard, A., Genter, A., Kohl, T., Lutz, P., Rose, P., Rummel, F. The deep EGS (enhanced geothermal system) project at Soultz-sous-Forêts (Alsace, France). *Geothermics* (2006), **35**(5), 473-483.

Hébert, R.L., Ledésert, B. Calcimetry at soultz-sous-forêts enhanced geothermal system: Relationships with fracture zones, flow pathways and reservoir chemical stimulation results. In: *Geothermal Energy, Technology and Geology* (2012), 93-113.

Hébert, R.L., Ledésert, B., Bartier, D., Dezayes, C., Genter, A., Grall, C. The enhanced geothermal system of soultz-sous-forêts: A study of the relationships between fracture zones and calcite content. *Journal of Volcanology and Geothermal Research* (2010), **196**(1-2), 126-133.

Hooijkaas, G.R., Genter, A., Dezayes, C. Deep-seated geology of the granite intrusions at the Soultz EGS site based on data from 5 km-deep boreholes. *Geothermics* (2006), **35**(5-6), 484-506.

Kohl, T., Mégel, T. Predictive modeling of reservoir response to hydraulic stimulations at the European EGS site Soultz-sous-Forêts. *International Journal of Rock Mechanics and Mining Sciences* (2007), **44**(8), 1118-1131.

Komninou, A., Yardley, B.W.D. Fluid-rock interactions in the Rhine Graben: A thermodynamic model of the hydrothermal alteration observed in deep drilling. *Geochimica et Cosmochimica Acta* (1997), **61**(3), 515-531.

Lasaga, A., Soler, J., Ganor, J., Burch, T., Nagy, K.. Chemical weathering rate laws and global geochemical cycles, *Geochimica et Cosmochimica Acta* (1994), **58**(10), 2361-2386.

Ledésert, B., Hebert, R., Genter, A., Bartier, D., Clauer, N., Grall, C. Fractures, hydrothermal alterations and permeability in the Soultz Enhanced Geothermal System. *Comptes Rendus - Géoscience* (2010), **342**(7-8), 607-615.

Ledésert, B., Hébert, R.L., Grall, C., Genter, A., Dezayes, C., Bartier, D., Gérard, A. Calcimetry as a useful tool for a better knowledge of flow pathways in the Soultz-sous-Forêts Enhanced Geothermal System. *Journal of Volcanology and Geothermal Research* (2009), **181**(1-2), 106-114.

Ledoux, E. Etude expérimentale d'un doublet hydrothermique : interprétation des expériences 'puits unique'. BRGM-Ecole des Mines de Paris, Paris (1978).

Ngo, V.V., Lucas, Y., Clément, A., Fritz, B. Modeling the impact of temperature on the saturation state and behavior of minerals in the Soultz-sous-Forêts geothermal. *Geothermics* (2016), accepted.

Pitzer, K.S., 1973. Thermodynamics of electrolytes. I. Theoretical basis and general equations. *Journal of Physical Chemistry* (1973), **77**(2), 268-277.

Portier, S., Vuataz, F.D., Nami, P., Sanjuan, B., Gérard, A. Chemical stimulation techniques for geothermal wells: experiments on the three-well EGS system at Soultz-sous-Forêts, France. *Geothermics* (2009), **38**(4), 349-359.

Rabemanana, V., Durst, P., Bächler, D., Vuataz, F.D., Kohl, T. Geochemical modelling of the Soultz-sous-Forêts Hot Fractured Rock systemcomparison of two reservoirs at 3.8 and 5 km depth. *Geothermics* (2003), **32**(4), 645-653.

Sanjuan, B., Pinault, J.L., Rose, P., Gérard, A., Brach, M., Braibant, G., Crouzet, C., Foucher, J.C., Gautier, A., Touzelet, S. Tracer testing of the geothermal heat exchanger at Soultz-sous-Forêts (France) between 2000 and 2005. *Geothermics* (2006), **35**(5-6), 622-653.

Sausse, J., Fourar, M., Genter, A. Permeability and alteration within the Soultz granite inferred from geophysical and flow log analysis. *Geothermics* (2006), **35**(5-6), 544-560.

Sauty, J.P., Gingarten, A.C., Menjoz, A., Landel, P.A. Sensible energy storage in aquifers; 1, Theroretical study. *Water Resources Research* (1982), **18**, 245-252.

Scheiber, J., Seibt, A., Birner, J., Genter, A., Moeckes, W. Application of a Scaling Inhibitor System at the Geothermal Power Plant in Soultz-sous-Forêts: Laboratory and On-Site Studies. In: *Proceedings of European Geothermal Congress*, Pisa, Italy (2013).

Acknowledgements

We are grateful to the financial support of the “LabEx G-EAU-THERMIE PROFONDE” program at the University of Strasbourg. We warmly thank Dr. Albert Genter and Dr. Julia Scheiber for their helpful and constructive comments, as well as for providing the experimental data related to the fluid chemistry.